

/THEORETICAL STUDY OF OSCILLATOR
STRENGTH IN HYPERSPHERICAL COORDINATES/

by

JIANG TAN
B.A., Cherkang University, 1976

A MASTER'S THESIS

submitted in partial fulfillment of the
requirements for the degree

MASTER OF SCIENCE

Department of Physics
KANSAS STATE UNIVERSITY
Manhattan, Kansas

1985

Approved by:

C. D. Lin

Major Professor

LD
2668
.T4
1985
T36
C.2

A11202 985566

ii

TABLE OF CONTENTS

	Page
TABLE OF CONTENTS	ii
LIST OF FIGURES	iii
LIST OF TABLES	iv
ACKNOWLEDGEMENTS	v
Chapter	
I. INTRODUCTION	1
II. REVIEW OF THE HYPERSPHERICAL COORDINATES METHOD . . .	3
III. OSCILLATOR STRENGTH	10
IV. NUMERICAL CALCULATIONS	15
V. DISCUSSION	37
1. Length Form vs. Acceleration Form	37
2. The Limitation of Adiabatic Approximation . . .	38
3. Future Direction	40
APPENDIX A	41
APPENDIX B	48
REFERENCES	54
ABSTRACT	

LIST OF FIGURES

Figure		Page
1	g-functions for H^- at $R=0.5, 6.0$, and 12 a.u.	16
2	Lowest $1S^e$ and $1P^0$ adiabatic potential curves of He	19
3	Lowest $1S^e$ and $1P^0$ adiabatic potential curves of H^-	21
4	Radial wave functions $F_{\mu E}$ for the three lowest states of the ground channel of He	23
5	Radial wave functions for the two lowest states of the $1P^0$ channel of He	25
6	Channel dipole moment densities D_{μ} of H^- and He as a function of hyperradius R in both $\mu\mu$ acceleration form and length form	28
7	Photoionization cross section of He	30
8	Photodetachment cross section of H^-	32
9	Comparison of ground state radial wave functions of H^- and He	34
A1	Coordinate system for a 2-electron system	42

LIST OF TABLES

Table	Page
I Comparison of energies for several states of He and H^- . . .	52
II Comparison of f values in length and acceleration forms . . .	53

ACKNOWLEDGEMENTS

I very much wish to thank Professor Ugo Fano, University of Chicago, who laid the foundations of my education in physics.

I would like to express my gratitude to Professor Chii-Dong Lin for his guidance and encouragement throughout the course of this work.

I extend thanks to the members of my advisory committee, Professor Talat Rahman and Professor Lew Cocke, for their interest in this work and many helpful discussions.

I especially thank Dr. Isao Shimamura for his valuable comments and suggestions concerning the contents of this work. Also, I want to thank Alexander Skutlartz for his care about this work being carried out. To my parents, my husband S. L. Lee, and sisters goes a very special thanks. Their love and support made my stay far from home possible. I also wish to express special thanks to my friend, Ping Yip.

I appreciate the expert typing of this thesis by KoKo Himes.

The financial support by the U.S. Department of Energy, Division of Chemical Sciences, is gratefully acknowledged.

Chapter I

INTRODUCTION

The oscillator strength f and photoabsorption cross section of He and H^- have been the subject of many theoretical and experimental investigations.^{1,2} The earlier theoretical calculations carried out to determine the photoionization cross sections of He using hyperspherical coordinate approach were due to Miller and Starace.³ In this work we calculated f values of bound-bound transitions of He, and the cross sections of photoionization of He and photodetachment of its isoelectronic system H^- in hyperspherical coordinates. Also, we extend previous length form calculation to an acceleration form (Appendix B) calculation aiming at judging if hyperspherical wavefunctions in the adiabatic approximation are accurate in certain regions of configuration space and of energy. The results show that the disagreement of length form and acceleration form is large with an estimated accuracy of 4-42% in H^- photodetachment for example. The acceleration form requires a more accurate wave function, and as such is subjected to rather large errors. Both the length and acceleration forms revealed a systematic error for large photoelectron energies. It is believed that adiabaticity of channels breaks down at high energies.

In fact, for one-electron processes, like the one investigated here, many theoretical calculations with better results have been carried out.² When employed in hyperspherical fashion the f values and cross sections obtained seem to have no advantage over other approaches. However the use of the hyperspherical approach has its own strength. Its particular merit

rises rather from the physical interpretation that can be given to the transition pattern. The power of this technique is apparent when double-excitation processes or more difficult situations ^{like under external fields} are attacked. Thus the attempt to achieve a detailed understanding of the systematic error of the adiabatic approximation and the improvement of the framework continues to provide an interesting task to hyperspherical coordinates formulation.

Chapter II

REVIEW OF HYPERSPHERICAL COORDINATES METHOD

The non-relativistic Schrodinger equation for two-electron systems is (atomic units are used throughout)

$$(-\frac{1}{2} \nabla_1^2 - \frac{1}{2} \nabla_2^2 - \frac{Z}{r_1} - \frac{Z}{r_2} + \frac{1}{r_{12}} - E) \psi(\vec{r}_1, \vec{r}_2) = 0 \quad (1)$$

where r_1 and r_2 are two electrons' distances measured from the nucleus, r_{12} is the distance between the electrons and Z is the nuclear charge. We know that the $SO(4)$ symmetry holds for an object moving in a potential proportional to $1/r$. For our system the existence of $1/r_{12}$ distorts the $SO(4)$ symmetry of independent particles. But still a regular pattern of energy spacing and width was observed in He photoabsorption spectrum.^{4,5} It is obvious that there exists a certain symmetry. Following this pattern, Rydberg series and their continua were grouped as 'channels'. Since a 'channel' is the mirror of the existence of certain symmetry, it would be specified by the radial joint motion of the two electrons approaching the nucleus (dynamical symmetry) and by the orbital angular momentum of their joint motion about the center of mass (geometrical symmetry).

Actually the interaction $1/r_{12}$ does not break the system's geometrical symmetry group $O(3)$ generated by the angular momentum L . Also the system's other $O(3)$ subgroup, the dynamical symmetry group, referred to as the 'hidden' symmetry group, is not totally broken. The system still retains some residual hidden symmetry. The conventional configuration interaction method cannot show this residual hidden symmetry. The hyperspherical approach introduced by Macek, Fano and Lin⁶ was aimed at treating the system in such a

way that the approximate symmetry property of the system would emerge so that the quantum numbers associated with each channel⁷ come out naturally.

The transformation to hyperspherical coordinates from the usual spherical coordinates is given by

$$R = (r_1^2 + r_2^2)^{1/2} \quad (2)$$

and

$$\alpha = \text{tg}^{-1} (r_1/r_2) \quad (3)$$

Thus spatial coordinates transform from $(r_1, r_2, \theta_1, \theta_2, \phi_1, \phi_2)$ to $(R, \alpha, \theta_1, \theta_2, \phi_1, \phi_2) \equiv (R, \Omega)$, and the kinetic energy of the system

$$-\frac{1}{2} \nabla_1^2 - \frac{1}{2} \nabla_2^2 \quad (4)$$

becomes

$$-\frac{1}{2} \left(\frac{\partial^2}{\partial R^2} + \frac{5}{R} \frac{\partial}{\partial R} - \frac{\Lambda^2}{R^2} \right) \quad (5)$$

where Λ^2 is a grand angular momentum operator (A.8).

The total Coulomb potential is C/R , where C is an effective nuclear charge (A.9). Under this transformation equation (1) becomes

$$\left[\frac{\partial^2}{\partial R^2} + \frac{5}{R} \frac{\partial}{\partial R} + \frac{1}{R^2} (-\Lambda^2 + RC) + 2E \right] \psi(R, \Omega) = 0 \quad (6)$$

To eliminate the first order derivatives with respect to R and to α , the wave function $\bar{\psi}(R, \Omega)$ can be renormalized by a factor $R^{5/2} \sin \alpha \cos \alpha$. The renormalized wave function $\bar{\bar{\psi}}(R, \Omega)$ satisfies

$$\int \bar{\bar{\psi}}^* \bar{\bar{\psi}} dR d\Omega = 1 \quad (7)$$

where

$$d\Omega = d\alpha \sin\theta_1 d\theta_1 d\phi_1 \sin\theta_2 d\theta_2 d\phi_2 \quad (8)$$

and the Schrodinger equation

$$\left[\frac{\partial^2}{\partial R^2} + \frac{1}{4R^2} - \frac{\Lambda^2}{R^2} + \frac{C}{R} + 2E \right] \bar{\psi}(R, \Omega) = 0 \quad (9)$$

The structure of the equation (9) is similar to the radial equation of H atom except that $[\Lambda^2, C] = \Lambda^2 C - C \Lambda^2 \neq 0$

It is worth noticing that the non-commutation of Λ^2 and C is responsible for the broken symmetry. If they commute we would get n^2 degeneracy of $SO(4)$ symmetry by the two generators $L = L_1 + L_2$ and a 'hyper-Lenz' vector defined like

$$\vec{A} = \frac{1}{2} (\vec{p} \times \vec{L} - \vec{L} \times \vec{p}) - \frac{\hat{R}}{R} \quad (10)$$

Of course this is not the case. Since $[\Lambda^2, C] \neq 0$, thus $[\vec{A}, H] \neq 0$, therefore \vec{A} is not a constant of motion hence not a Lenz vector. The non-commutation of Λ^2 and C also makes $\bar{\psi}$ not totally separable in this coordinate. However, we can approach the solution by first solving the adiabatic ($\frac{\partial}{\partial R} = 0$) equation

$$H_{R=CONST} \phi_\mu(R; \Omega) = U_\mu(R) \phi_\mu(R; \Omega) \quad (11)$$

at each value of R , i.e., R is treated as a parameter. The eigenvalues U are discrete; their corresponding eigenfunctions furnish a complete set $\{\phi_\mu\}$, where μ is the label of each base ϕ . Performing the expansion of the wave function ψ (where we have dropped the bar) in terms of such a complete set

$$\psi_\nu(R, \Omega) = \sum_\mu F_{\nu\mu}(R) \phi_\mu(R; \Omega) \quad (12)$$

We then obtain from the Schrodinger equation (9) a set of coupled equations

$$\left\{ \frac{d^2}{dR^2} + \frac{1}{4R^2} + U_\mu(R) + 2E \right\} F_{\mu\mu}(R) + \sum_{\mu'} W_{\mu\mu'}(R) F_{\mu'\mu}(R) = 0 \quad (13)$$

$$W_{\mu\mu'} = \left(\phi_\mu, \frac{\partial^2}{\partial R^2} \phi_{\mu'} \right) + 2 \left(\phi_\mu, \frac{\partial}{\partial R} \phi_{\mu'} \right) \frac{d}{dR} \equiv (P^2)_{\mu\mu'} + 2P_{\mu\mu'} \frac{d}{dR} \quad (14)$$

If we set the coupling term $W_{\mu\mu'} = 0$, it admits a wave function of the form

$$\Psi_\nu(R, \Omega) = F_\nu(R) \phi_\nu(R; \Omega) \equiv \Psi_\nu^{\text{ad}}(R, \Omega) \quad (15)$$

where the superscript 'ad' stands for 'adiabatic' and functions $F_\mu(R)$ and ϕ_μ satisfy, respectively, equations

$$-\frac{1}{R^2} (-\hbar^2 + RC) \phi_\mu = U_\mu(R) \phi_\mu \quad (16)$$

and

$$\left\{ \frac{d^2}{dR^2} - U'_\mu(R) + 2E \right\} F_\mu(R) = 0 \quad (17)$$

where

$$U'_\mu(R) = U_\mu(R) + \frac{1}{4R^2} + W_{\mu\mu}(R) \quad (18)$$

We see that equation (16) is an adiabatic channel equation (11). The second equation (17) describes the motion of a pair of two electrons as one particle in the central potential $U(R)$. We have therefore first transformed the original two-electron problem to a problem of one particle moving in a six-dimensional hyperspace, and then 'quasi-decoupled' the motion into two parts, namely, that of the one-dimensional radial motion of a single electron pair and that of the five-dimensional correlated angular motion of the pair which depends on the hyperradius R parametrically.

The solution $F(R)$ of equation (17) is a typical one-particle-type radial function. ϕ is, on the other hand, a two-particle function which is properly symmetrized under interchange of electrons one and two:

$$\phi_{\mu}(1,2) = (1 \pm P_{12}) \sum_{\ell_1 \ell_2} g_{\ell_1 \ell_2}^{\mu}(1,2) Y_{\ell_1 \ell_2 LM}(1,2) \quad (19)$$

In Equation (19), P_{12} is the permutation operator, ℓ_1, ℓ_2 are chosen to give L and π symmetry, and the singlet and triplet states are associated with the inclusion of the plus or minus sign, respectively. $g_{\ell_1 \ell_2}^{\mu}$ are functions of α , which change gradually with R , and the function $Y_{\ell_1 \ell_2 LM}$ are the usual coupled spherical harmonics.

$$Y_{\ell_1 \ell_2 LM}(1,2) = \sum_{m_1 m_2} Y_{\ell_1 m_1}(1) Y_{\ell_2 m_2}(2) \langle \ell_1 m_1 \ell_2 m_2 | L, M \rangle \quad (20)$$

The function ϕ_{μ} is the channel function for channel μ where $\mu = (N, (K, T)^A, L, S, \pi)$ a collective quantum number as given by Lin.⁷ From a given channel potential $U_{\mu}(R)$ the radial function $F_{\mu}(R)$ which specifies each state in the Rydberg series or in the continuum is obtained from (17).

A few more remarks about this method are desirable before ending this section. Firstly, we have mentioned at the beginning that the hyperspherical approach would show the residual $SO(4)$ symmetry of the system. We know that the central potential $V(r)$ leads to invariance of L ; in the mean time, if $V(r)$ also has $1/r$ form, this would lead to another dynamical invariance, the invariance of Lenz vector. Note that the dynamical quantum numbers (K, T) assigned to a channel suggested by Lin⁷ are not exact quantum numbers.

Secondly, our system has been treated within the adiabatic approxima-

tion, $W_{\mu\mu} = 0$. This is equivalent to

$$\psi_E = \psi_E^{\text{ad}} = F_{E\mu}(R)\phi_\mu(R;\Omega) \quad (21)$$

$$E = E_\mu \quad (22)$$

Here the adiabatic channel function ϕ_μ is the zeroth order eigenfunction of the Hamiltonian H ; adiabatic channel energy E_μ is the zeroth order approximation to the exact energy. We see that the interaction between the states can appear explicitly only through the coupling terms $W_{\mu\mu}$. Keeping in mind the usual configuration interaction picture, one might raise a question: Since there are no 'interchannel interactions', say, $F_\mu(E)$ and $F_\mu(E')$, if we ignore the 'interchannel interaction' $W_{\mu\mu}$, is this adiabatic approximation ($W_{\mu\mu} = 0$) identical to an independent particle approximation? The answer is no, because the hyperspherical framework is based on a fundamentally different picture. We seek to describe the motion of electrons in terms of the coupled coordinates (R, α) which emphasize directly the correlation between the two electrons. Thus almost all the interactions between the two electrons are already included in the calculations of ϕ_μ . Hence the treatment rests on small deviation of the adiabatic solution from the exact one. The magnitude of the deviation would be seen by examining the energy, if bound, or the phaseshift, if unbound, obtained from the adiabatic calculation. Energies and phase shifts calculated by approximate wave functions contain only errors of second order in the error in the wave function. Therefore, even an inaccurate wave function can produce a reasonably good energy or phase shift. On the other hand the error in the oscillator strength is of the first order in the error in the wave function. Thus, oscillator-strength calculations will provide a much more stringent test of

the wave function.

Traditionally, attempts to judge the accuracy of computed f values have resorted to the argument among the agreement of 'length', 'velocity' and 'acceleration' forms of f values (Appendix B). These various forms of the f would be equivalent if the exact wave functions were employed, but will generally disagree when computed with approximate wave functions. We can employ this criterion to judge if hyperspherical wave functions are accurate, or at least if they are adequate in the regions of configuration space (r_1, r_2) which are important for the oscillator strength. We know that an approximate wave function chosen from an energy-minimization may be considerably different from the true function.

Chapter III OSCILLATOR STRENGTH

This section is devoted to the calculation of the oscillator strength f and photoabsorption cross section.

f is a quantum mechanical quantity derived from the classical model of polarizability of atoms. It is introduced customarily in discussions of transition intensities. For a state-to-state transition it is defined as (a.u.)

$$f_{ka} = \frac{2}{3} \omega_{ka} |\langle \Psi_k | \sum_i \vec{r}_i | \Psi_a \rangle|^2 \quad (23)$$

where Ψ_a is the initial state and Ψ_k is the final state, ω_{ka} is the energy difference between the two states. For a single-electron system $f_{ka} = f_{n\ell m, n'\ell' m'}$, where m and m' refer to a given choice of z -axis. In practice, the measurement of transition intensity would deal with transitions to all final states of equal energy E_k and different orientations. Moreover, the atoms in the initial states in general have random orientation in which case averaging of f over all initial states of different orientations is required. Thus it is convenient to define an average oscillator strength by averaging over degenerate initial states Ψ_a and sum over the orientation of final states Ψ_k :

$$\bar{f}_{\bar{k}\bar{a}} = \frac{1}{2L_a + 1} \sum_{M_k, M_a} f_{ka} \quad (24)$$

where \bar{k} and \bar{a} denote all the quantum numbers needed to define a state other than magnetic quantum number M . For single-electron systems it is

$$f_{n'l',nl} = \frac{1}{2l+1} \sum_{m',m} f_{n'l'm',nlm} \quad (25)$$

Equation (26) can be rewritten as

$$f_{ka} = \frac{2\omega_{ka}}{2l_a+1} |\langle \psi_k | \sum_i z_i | \psi_a \rangle|^2 \quad (26)$$

In the ionization processes, that is, for states k in the continuous spectrum, the wave function ψ_k is chosen to be 'energy normalized' and oscillator strength (24) is represented by df/dE_k .

The expression for f given in (26) is called the length form. Alternative expressions of f exist, in terms of matrix elements of the electron velocity, acceleration, etc.

$$f_{vel} = \frac{2}{2l_a+1} \frac{1}{\omega_{ka}} |\langle \psi_k | \sum_i (P_z)_i | \psi_a \rangle|^2 \quad (27)$$

$$f_{acc} = \frac{2}{2l_a+1} \frac{Z}{\omega_{ka}} |\langle \psi_k | \sum_i \frac{z_i}{r_i^3} | \psi_a \rangle|^2 \quad (28)$$

These expressions are derived from (26) by means of operator transformation in Appendix B.

The main purpose of this thesis is to calculate the oscillator strength for bound-bound transitions of He, and the photoionization and the photo-detachment cross sections of He and H^- , respectively, using wave functions calculated in hyperspherical coordinates. In terms of the length form and the wave functions given by (21),

$$\begin{aligned} f_{len} &= 2\omega |\langle \psi_\mu | z_1 + z_2 | \psi_\mu \rangle|^2 \\ &= 4\omega |\langle \psi_\mu | z_1 | \psi_\mu \rangle|^2 \\ &= 4\omega \left| \int dR F_{\mu E}(k) R F_{\mu E}(R) \int d\Omega \phi_\mu \sin \alpha Y_{10}(1) \phi_\mu \right|^2 \\ &= 4\omega |\langle F_{\mu E}(R) | R D_{\mu\mu}^2 | F_{\mu E}(R) \rangle|^2 \end{aligned} \quad (29)$$

where F_{μ} and $F_{\mu'}$ are radial wave functions of the initial and final states, respectively, with energy difference $E_{\mu} - E_{\mu'}$ equal to the photon energy ω .

$D_{\mu\mu'}(R)$ is 'channel dipole moment density'

$$D_{\mu\mu'}^{\ell} = (\phi_{\mu} | \sin \alpha Y_{10}^{(1)} | \phi_{\mu'}) \quad (30)$$

where the symbol $()$ denotes integration over all the angles Ω , $Y_{10}^{(1)}$ is the usual spherical harmonic function with angular coordinates of electron 1. The explicit expression of D is given in Appendix B. The quantity D represents the density of the 'angular' part of the dipole matrix element as a function of the size R of the system.

Similarly, working in the acceleration form we write f as

$$\begin{aligned} f_{\text{acc}} &= \frac{2}{\omega^3} \left| \langle \psi_{\mu} | \frac{Z}{r_1^3} + \frac{Z}{r_2^3} | \psi_{\mu'} \rangle \right|^2 \\ &= \frac{4Z}{\omega^3} \left| \langle F_{\mu} E(R) | \frac{1}{R^2} D_{\mu\mu'}^a | F_{\mu'} E(R) \rangle \right|^2 \end{aligned} \quad (31)$$

where Z is the nuclear charge and

$$D_{\mu\mu'}^a = (\phi_{\mu} | \frac{Y_{10}^{(1)}}{\sin^2 \alpha} | \phi_{\mu'}) \quad (32)$$

is the channel dipole moment density in acceleration form.

Oscillator strength in velocity form is not attempted in this work because it requires the derivative of the wave functions which makes the calculation much too complicated.

In general, the extent of departure of the approximate wave function from an exact one in different configuration space depends on the nature of the approximate wave function. Thus when we employ different f forms the error of the wave function contributes to the f -value calculations differently. Comparing with the two forms in the hyperspherical coordinate the length form

would be less prone to error. The reason is as follows.

At the boundary $R=0$ and at $\alpha=0$, and $\alpha=\pi/2$ the wave function density is required to be zero. Near these boundaries the wave function calculated is not accurate because of its very small amplitude at these regions. According to (31), the acceleration form puts a heavier weight at these inaccurate regions. The factor $1/R^2$ in the radial integral as well as the factor $\frac{1}{\sin^2 \alpha}$ in the angular integral introduced removable singularities at $R=0$ and $\alpha=0$. Thus the exact amplitudes of $\Psi(R, \alpha)$ near boundaries become very important. On the other hand, the length form has factors R and $\sin \alpha$ which leads to a third-order zero at boundaries. The inaccuracy of wave functions at small- R and small- α regions becomes less important. Since acceleration form picks up the 'wrong' regions of $\Psi(R, \alpha)$ we expect that the result of f value from the acceleration form calculation would be less reliable.

There is a great advantage of this method. The oscillator strengths were calculated by isolating $D_{\mu\mu}$, from the whole transition moment. $D_{\mu\mu}$, deserves its name 'channel dipole moment density' because it is characteristic of the entire Rydberg series, not of a particular state-to-state transition. We have already seen that all the important properties of electron correlation are contained in the channel function ϕ . The angular integral part of the f calculation, $D_{\mu\mu}$, is therefore of great importance in discussing radiative transitions. The functions $D_{\mu\mu}(R)$ offer a rough representation of the oscillator strength distribution among the transitions between different channels. It will exhibit whether the transition from one channel to another is favored or not. On the other hand, the information of f value for each particular transition line is contained in the overlap of $F_{\mu}(R)$ and $F_{\mu'}(R)$ with the weight of $D_{\mu\mu'}(R)$. These energy-

dependent radial integrals determine the relative oscillator strengths for states within the channel which are always non-zero as long as $D_{\mu\mu}$ is non-zero. On the other hand, the angular integrals are only non-zero for particular symmetry changes of the initial and the final channels, giving rise to selection rules. In this paper, we consider the manifold of dipole transitions from S states in the photon energy region where only single excitation channels (channels corresponding to the first ionization limit) are energetically accessible. Thus the non-zero $D_{\mu\mu}$ is from $1s^e$ channel to $1p^o$ channel. However, if we extend photon energy up to open double-excitation channels, $N=2$ for instance, there are three channels which have $1p^o$ symmetry. In the usual independent particle classification these channels correspond to $2snp\ 1p^o$, $2pns\ 1p^o$ and $2pnd\ 1p^o$. The experimental spectrum 5 showed that one Rydberg series had strong intensity and one Rydberg series was very weak. The third possible series was not observed. All these channels have identical L, S, and π and thus the selection rules for L, S, and π are not enough. It would be desirable to see if the relative magnitude of $D_{\mu\mu}$ among these channels can explain these experimental results. Such results would also give approximate selection rules for radiative transitions in terms of dynamical quantum numbers. In our single excitation case here, such dynamical information will not show. Actually, using hyperspherical wave functions to calculate f value for single excitation is to test the method aiming at future further work in double excitations.

Another advantage is that when we deal with the calculations including many energy states, hyperspherical wave functions have offered a much simpler method which involves the major part of the calculation only once for all energies. The rest of the calculation for each transition is very simple.

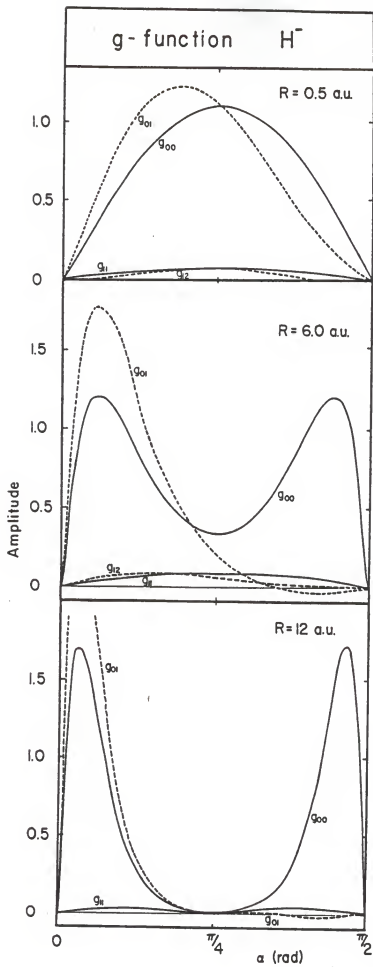
Chapter IV

NUMERICAL CALCULATIONS

In this section, we discuss the computational procedure for calculating oscillator strengths and photoabsorption cross sections using the wave functions calculated in hyperspherical coordinates. First we solved Eq. 16. The adiabatic Hamiltonian $H(R = \text{const.})$ was formed and diagonalized in the basis functions of hyperspherical harmonics $F_{\ell_1 \ell_2 \mu}(\alpha)$ which are the eigenfunctions of the Λ^2 operator (Appendix A, Eq. 23), and analytical channel functions⁹, at several values of R from $ZR=0.5$ to $ZR=14$. The basis set of as small as four or six functions for each of the three (ℓ_1, ℓ_2) pairs were combined to give three partial channel functions $g_{\ell_1 \ell_2 \mu}$. The three pairs were (ss), (pp), and (dd) for $1S^e$ and (sp), (pd), and (df) for $1P^o$. Thus the channel functions ϕ of the form Eq. (B.8) for $1S^e$ and Eq. (B.9) for $1P^o$ were constructed and the channel potentials (adiabatic potential) were obtained. As an example of the structures of channel functions ϕ_μ , several partial channel functions $g_{\ell_1 \ell_2 \mu}$ of H^- are given in Fig. 1 for small R , intermediate R , and large R . Comparing these three graphs we could see that at small R g has large amplitude around $\alpha \sim \pi/4$, i.e., the two electrons tend to be at equal distances from the nucleus when the size of the system is small; at large R , $g_{\ell_1 \ell_2 \mu}$ is squeezed into the boundary region of α ($\alpha=0$ or $\alpha=\pi/2$) from the middle region corresponding to that one electron is close to the nucleus and the other far away from it. The evolution of $g_{\ell_1 \ell_2 \mu}$ with R mirrors how the configuration of the system (r_1, r_2) changes as the size of the system R changes from the strongly correlated region to

Figure 1: g -functions for H^- at $R=0.5, 6.0$, and 12 a.u.

———— $g_{\ell_1 \ell_2}$ of ground channel
----- $g_{\ell_1 \ell_2}$ of excited $1p^0$ channel



the independent particle region. In the graph we could notice that after R greater than 6, $g_{\ell_1 \ell_2 \mu}$ began to have a node. These numerical errors came from the 2snp analytical channel function which was used as one of the basis functions in the calculations of $1p^0$ channel. It becomes non-negligible as R becomes large and it has a node and a small negative tail.

In Fig. 2 the lowest potential curve for $1s^e$ and for $1p^0$ are shown for He. The corresponding curves are shown for H^- in Fig. 3. They are similar to those displayed in Fig. 2 except that the $1p^0$ curve is repulsive. Within the adiabatic approximation, the bound state as well as continuum state wave functions $F(R)$ were calculated by solving Eq. (17). The resulting lowest bound state radial wave functions $F(R)$ of He are shown in Fig. 4 for $1s^e$ and Fig. 5 for $1p^0$. We could see that the nodal structure is the same as that of hydrogen radial wave function. For continuum state we normalize the wave functions according to

$$\int F_{\epsilon' \mu'}(R) F_{\epsilon \mu}(R) dR = \delta_{\mu \mu'} \delta(\epsilon - \epsilon') \quad (33)$$

The lowest bound state energies of He obtained using the present approach are compared in Table I with the energies obtained by Pekeris *et al.*¹⁰ In the latter calculation extensive variational methods with a few hundred parameters was used. So far we have seen that the energy levels calculated by hyperspherical wave functions agree well with those obtained by the large-scale calculations. For H^- , there is only one bound state. This ground state energy calculated in hyperspherical coordinates is -1.0508 Ry, with an accuracy of 0.44% compared with experimentally determined -1.0555 Ry.¹¹ These bound-state energies of He and H^- are also indicated in Fig. 2 and Fig. 3, respectively. Following the usual independent particle notation, these levels are labelled by $(n_1 \ell_1, n_2 \ell_2)$.

Figure 2: The lowest $1S^e$ and $1P^0$ adiabatic potential curves of the He. Energies calculated using these potentials are shown in horizontal lines.

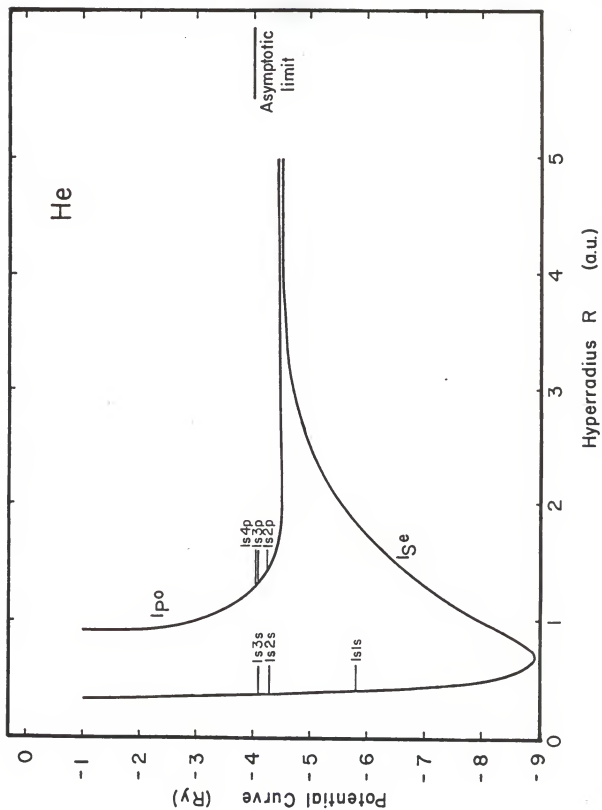


Figure 3: The lowest $1s^e$ and $1p^o$ adiabatic potential curves of H^- .

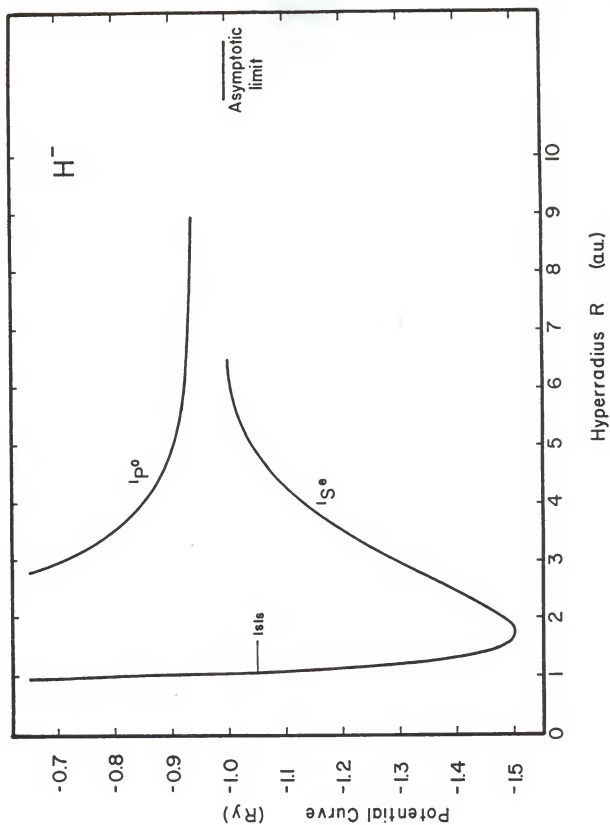


Figure 4: Radial wave functions $F_{\mu E}$ for the three lowest states of the ground channel of He.

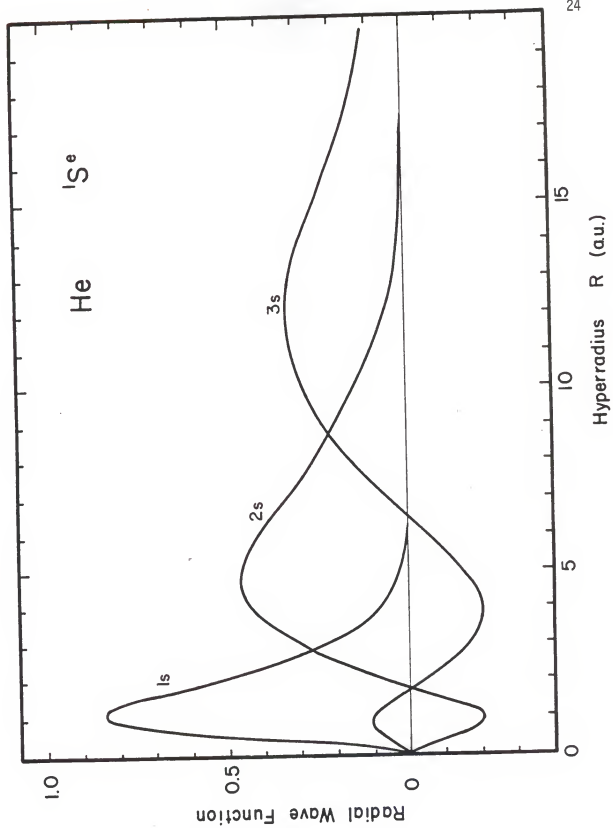
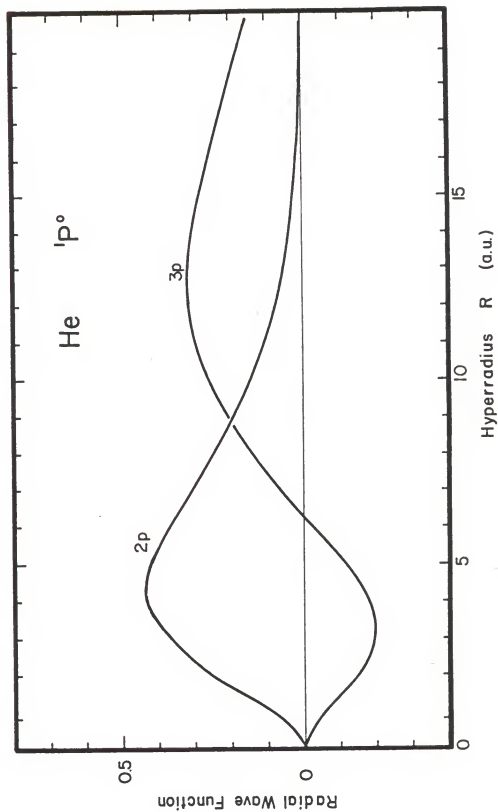


Figure 5: Radial wave functions for the two lowest states of the $1p^0$ channel of He.



Having obtained channel functions ϕ_s and ϕ_p , we calculated the channel dipole moment density $D_{sp}(R)$ in both length and acceleration forms for He and H^- . The asymptotic values of $D_{sp}(R)$ at large R for both length and acceleration forms were calculated using a single analytical basis function with $(\ell_1, \ell_2) = (0, 0)$ for $1s^e$ and $(\ell_1, \ell_2) = (0, 1)$ for $1p^0$, since couplings with other (ℓ_1, ℓ_2) pairs are negligible in this limit. The asymptotic values of $D_{sp}(R)$ are identical for He and H^- if reduced length scale ZR is used. The results of the length and acceleration forms for $D_{sp}(R)$ are shown in Fig. 6. From the figure, we notice that the length form of $D(R)$ is almost independent of R , while that in acceleration form it varies significantly with R . The final results of length and acceleration formulations for the photoionization (or photodetachment) of He and H^- are compared with experiment^{12,13} in Figures 7 and 8, respectively.

From the results exhibited in the figures of cross sections, we notice that the disagreement between length and acceleration forms in continuum transitions are large. It is about 4-42% in the case of H^- . The result for He is better. This is because H^- is very weakly bound, and an elaborate channel wave function ϕ_μ is necessary to reproduce well the potential $U_\mu(R)$ and hence $F(R)$. In Fig. 9 two ground radial wave functions of He and H^- are plotted together in scaled size ZR to show that the wave function of H^- is very diffuse. Also, our result shows that the cross section at higher energy becomes too small for both length and acceleration forms.

Our results of cross section both for He and H^- are in agreement with the recent calculations done by Park and Starace (private communication).

The f values of He photoexcitation are presented in Table II. From Table II we note that in the length form the f values for the excitation from ground state are reasonably good. But those values become inaccurate

Figure 6: The channel dipole moment densities $D_{\mu\mu}$, of H^- and He as a function of hyperradius R in both acceleration form and length form.

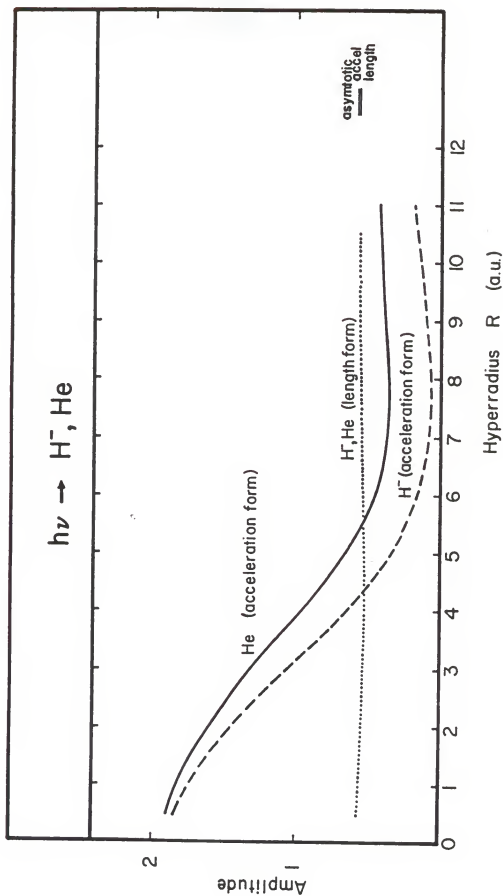


Figure 7: The photoionization cross section of He. The solid line is the result of an acceleration form calculation. The dashed line is the length form, and the dotted line is the experimental result by J. Samson.¹²

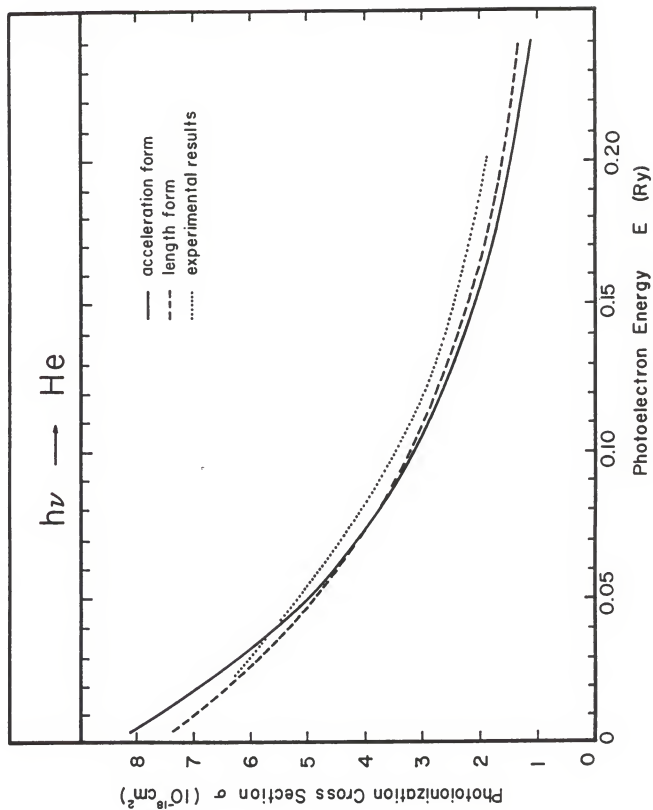


Figure 8: The photodetachment cross section of H^- calculated using the adiabatic approximation in both length form and acceleration form, compared with the experimental results of Smith and Burch.¹³

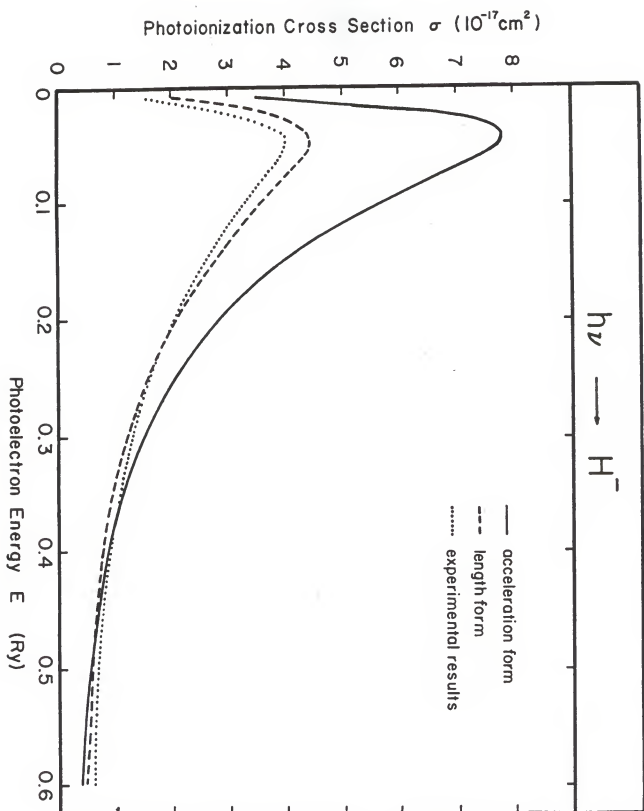
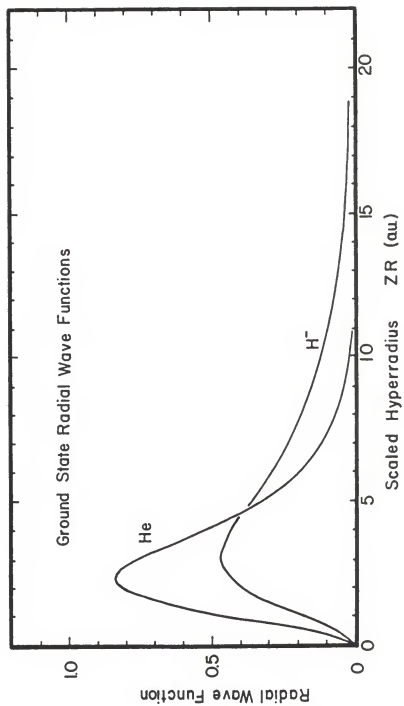


Figure 9: The comparison of ground state radial wave functions of H^- and He. The radial wave functions are plotted against the hyperradius R to a charge-reduced scale.



as initial state energy increases. The f values calculated from acceleration form are not as good as those from length form and f values for the excitation from excited initial state are not displayed in the table because the errors of the results exceed the acceptable scale. The reason for these bad results is that the $\frac{1}{(\Delta E)^3}$ factor (Eq. 31) makes the f calculation very sensitive when ΔE is very small (e.g. for 3s-3p, $\frac{1}{(\Delta E)^3} = 9 \times 10^5$).

Chapter V

DISCUSSION

In this section we discuss the merits and problems of calculating oscillator strengths using hyperspherical coordinates. This discussion will be divided into two parts: (1) the difference of oscillator strength in length form and in acceleration form; and (2) the limitation of adiabatic approximation employed in the present study.

1. Length Form vs. Acceleration Form

According to the derivation of Appendix B, the oscillator strength can be calculated using different forms. If exact wave functions are used, the result calculated from the acceleration form should agree with that obtained from using the length form.¹⁹ When working in hyperspherical coordinates the acceleration form has disadvantages. In the acceleration form, Eq. (31), α and R dependence of the operator are inverse square power. This coordinate dependence puts more weight on small- α and small- R regions where both $\psi(^1S)$ and $\psi(^1P)$ are relatively inaccurate because of their very small amplitudes. In the small- R region radial function $F(R)$ is inadequate.¹⁴ To represent this region more accurately, a Fock expansion (Appendix A) is necessary. In the small- α region the channel function ϕ again does not represent the wave function very well. In this region the configuration of the system corresponds to that one electron is near the nucleus while the other one is far away, the correlation effect is essentially zero, so that the advantage of hyperspherical wave functions is lost. On the other hand, the small- α and small- R regions are not very important for the length form. Thus we tend to conclude

that the result obtained from the acceleration form is less reliable. And the disagreement between the two forms basically is not because of the poor quality of the whole wave function employed. Rather, it is due to the poor quality of the wave function in a limited range?

2. The Limitation of Adiabatic Approximation

In this work, we have used the adiabatic approximation in calculating both initial and final state wave functions. Our treatment rests on the adiabaticity of the two-electron system. The quasi-separability of R and Ω assumes that the true wave function is predominantly adiabatic wave function. That is, the expansion of ϕ in the base of $\{\phi_\mu\}$, Eq. (12), would be

$$\psi_\mu(R, \Omega) = \sum_\mu F_{\mu\mu} \phi_\mu = \psi_\mu^{\text{ad}} + \sum_{\mu' \neq \mu} F_{\mu\mu'} \phi_{\mu'} \quad (34)$$

where ψ_μ^{ad} is the leading term and the off-diagonal terms $F_{\mu\mu'}(R)$ are small functions in the sense that $|F_{\mu\mu'}|^2$ is small.

The adiabatic approximation is to neglect all the $F_{\mu\mu'}(R)$. In general, the adiabaticity of the system becomes less valid as the energy of the system increases. In our work we see that from Figs. 7 and 8 the cross section at higher energy becomes too small for both length and acceleration forms. Also, the f values shown in Table II become less accurate rapidly as initial state energy increases. The reason is that the quantum defects and the phase shifts calculated under our approximation are getting smaller monotonically as the energy increases. The adiabatic approximation is responsible for this systematic error. These can be attributed to the inadequacy of adiabatic approximation at higher energies. To get more accurate results systematic improvement of wave functions for states of high excitation energy is needed. To this end, one can go beyond the adiabatic approximation by

including more terms in the wave function expansion.

The neglect of all the $F_{\mu\mu}(R)$, or all the other channels ϕ_{μ} , is equivalent to setting the channel couplings $W_{\mu\mu}$, equal to zero. In principle, $F_{\mu\mu}(R)$ can be taken into account by solving the set of coupled equations.¹³ However, the previous work of Lin¹⁵ in calculating e-H scattering phase shifts using coupled equations shows that the rate of convergence is very slow. The same conclusion has been found by Starace in He photoabsorption cross sections.¹⁶ Thus, there could be a limitation in the hyperspherical method. The limitation stems from the diverging number of channels required in the coupled equations¹³ at higher energies. Therefore, in this work we did not try to improve our results along this line of approach.

The reason for the slow convergence of the number of channels required is that at high E , or more directly, large R the system goes to the fragmentation limit. In this limit the adiabatic channel function as a complete set $\{\phi_{\mu}\}$ is not a suitable basis for the total wave function. In other words, in this limit the physically appropriate coordinates are the independent particle coordinates. It is thus better to write wave functions in terms of the independent particle approximation. On the other hand, in the small- R region where the two electrons are strongly correlated, the hyperspherical coordinates have an advantage over the independent particle coordinates. Thus it would be desirable to employ hyperspherical coordinates in the internal region (small R) and match the solution to the external region (large R) where the wave functions are expressed in independent particle coordinates. So far this method has not been implemented. Also, there is a 'post-adiabatic' method developed by Klar and Fano¹⁷ which in principle can overcome the difficulty even though mathematically not simple. Develop-

ments in the field are still going on, and the wider applicability of the method is still to be proved.

3. Future Direction

Because of the importance of oscillator strength data in the laboratory plasma physics and in stellar astronomy, many theoretical methods have been developed to calculate f values. In this work we calculated oscillator strength and photoabsorption cross sections using hyperspherical coordinates. However, accurate determination of these data is not our present goal as we used only first order wave functions in the adiabatic approximation. In spite of the fact that the results are not very favorable, the method does provide deeper insight into the correlations of two electrons. For the study of transitions to doubly excited states, the present method would become much more appealing than other methods. Since there are many channels converging to a given threshold for doubly excited states, with the help of the classification scheme for these states, this method can identify which channels are important for photoabsorption. The dipole matrix density given in Eq. (30) should provide such information. Investigation of this type, both experimental and theoretical, are not yet available.

APPENDIX A

I. Schrodinger Equation

The nonrelativistic Schrodinger equation for two-electron systems is

$$\left(-\frac{1}{2}\nabla_1^2 - \frac{Z}{r_1} - \frac{1}{2}\nabla_2^2 - \frac{Z}{r_2} + \frac{1}{r_{12}} - E\right)\psi = 0 \quad (1)$$

In hyperspherical coordinates (R, α) defined by (see Fig. A.1)

$$r_1 = R \sin \alpha \quad (2)$$

$$r_2 = R \cos \alpha \quad (3)$$

where R is the mean-square radius of the two electrons, and α is the measure of the ratio of the magnitudes r_1 and r_2 . From

$$\frac{\partial}{\partial r_1} = \frac{\partial R}{\partial r_1} \frac{\partial}{\partial R} + \frac{\partial \alpha}{\partial r_1} \frac{\partial}{\partial \alpha} = \sin \alpha \frac{\partial}{\partial R} + \frac{\cos \alpha}{R} \frac{\partial}{\partial \alpha} \quad (4)$$

$$\frac{\partial}{\partial r_2} = \cos \alpha \frac{\partial}{\partial R} - \frac{\sin \alpha}{R} \frac{\partial}{\partial \alpha} \quad (5)$$

the Schrodinger equation in hyperspherical coordinates takes the form

$$\left(\frac{\partial^2}{\partial R^2} + \frac{5}{R} \frac{\partial}{\partial R} - \hat{U}(R, \alpha) + 2E\right)\psi(R, \alpha) = 0 \quad (6)$$

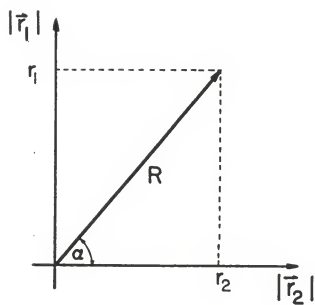
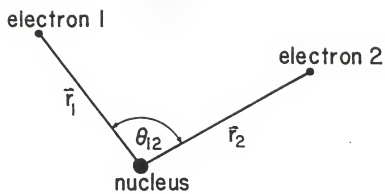
where

$$\hat{U} = \frac{1}{R^2} (\hat{\Lambda}^2 - RC) \quad (7)$$

is the effective potential operator

where

Figure A1: Coordinate system for a 2-electron system.



$$\begin{aligned}
\Lambda^2 &= - \left(\frac{\partial^2}{\partial \alpha^2} + \operatorname{ctg} 2\alpha \frac{\partial}{\partial \alpha} \right) + \frac{\ell_1^2}{\sin^2 \alpha} + \frac{\ell_2^2}{\cos^2 \alpha} \\
&= - \frac{1}{\sin^2 \alpha \cos^2 \alpha} \frac{\partial}{\partial \alpha} \sin^2 \alpha \cos^2 \alpha \frac{\partial}{\partial \alpha} + \frac{\ell_1^2}{\sin^2 \alpha} + \frac{\ell_2^2}{\cos^2 \alpha}
\end{aligned} \quad (8)$$

and

$$\begin{aligned}
C &= R \left(\frac{2Z}{r_1} + \frac{2Z}{r_2} - \frac{2}{r_{12}} \right) \\
&= \frac{2Z}{\sin \alpha} + \frac{2Z}{\cos \alpha} - \frac{2}{(1 - \sin 2\alpha \cos \theta_{12})^{1/2}}
\end{aligned} \quad (9)$$

is the effective Coulomb charge.

We can eliminate the first-order derivative of R by introducing a wave function

$$\Psi = R^{5/2} \psi \quad (10)$$

Thus wave function ψ satisfies the equation

$$\left(\frac{\partial^2}{\partial R^2} - \hat{U}(R, \Omega) + \frac{1}{4R} + 2E \right) \psi(R, \Omega) = 0 \quad (11)$$

The Schrodinger equation is not completely separable in these coordinates because the potential operator \hat{U} depends upon both R and Ω , and Λ^2 does not commute with C .

The wave function ψ can be expanded in terms of the eigenfunctions of \hat{U} at each R value

$$\psi = \sum_{\mu} F_{\mu}(R) \phi_{\mu}(R; \Omega) \quad (12)$$

where ϕ_{μ} are eigenfunctions of potential operator \hat{U} with eigenvalues U_{μ}

$$\hat{U}(R, \Omega) \phi_{\mu}(R; \Omega) = U_{\mu}(R) \phi_{\mu}(R; \Omega) \quad (13)$$

and $F_{\mu}(R)$ is the expansion coefficient.

Equation (13) is also the adiabatic representation of the original Schrodinger equation, namely

$$H_{R=\text{const}} \phi_{\mu}(R; \Omega) = -U_{\mu}(R) \phi_{\mu}(R; \Omega) \quad (14)$$

Substituting (12) to (11), premultiplying by ϕ_{μ} , and integrating over Ω leads to coupled equations

$$\left\{ \frac{d^2}{dR^2} - U_{\mu}(R) + \frac{1}{4R^2} + 2E \right\} F_{\mu} + \sum_{\mu'} W_{\mu\mu'}(R) F_{\mu'} = 0 \quad (15)$$

where

$$\begin{aligned} W_{\mu\mu'} &= (\phi_{\mu}, \frac{\partial^2}{\partial R^2} \phi_{\mu'}) + 2(\phi_{\mu}, \frac{\partial \phi_{\mu'}}{\partial R}) \frac{d}{dR} \\ &= (p^2)_{\mu\mu'} + 2p_{\mu\mu'} \frac{d}{dR} \end{aligned} \quad (16)$$

The problem of solving the Schrodinger equation for two electrons therefore reduces to that of solving the angular equation (13) at each R and the radial one-dimensional equation (15). In a practical numerical integration of equation (15), we can neglect the coupling term $W_{\mu\mu'}$. Then the radial equation (15) is simply

$$\left\{ \frac{d^2}{dR^2} - U_{\mu}(R) + 2E \right\} F_{\mu}(R) = 0 \quad (17)$$

where

$$U_{\mu}(R) = U_{\mu}(R) - \frac{1}{4R^2} - W_{\mu\mu}(R) \quad (18a)$$

and the diagonal term of $W_{\mu\mu}$, is

$$W_{\mu\mu} = p_{\mu\mu}^2 \quad (18b)$$

since ϕ_μ is real $P_{\mu\mu} = 0$. Also $P_{\mu\mu}^2$ is positive definite. Thus this term would always provide a positive energy shift. Back to equation (11) for the solution of $U_\mu(R)$, the first-order derivative with respect to α can be eliminated. Equation (13) is equivalent to

$$\left\{ -\frac{\partial^2}{\partial \alpha^2} + \frac{\ell_1^2}{\sin^2 \alpha} + \frac{\ell_2^2}{\cos^2 \alpha} - RC \right\} \frac{1}{R^2} \sin \alpha \cos \alpha \phi(R; \Omega) = 0 \quad (19)$$

In what follows we shall define $\sin \alpha \cos \alpha \phi$ to be channel function ϕ . This equation can be solved numerically by the basis sets of eigenfunctions of the asymptotic operator \hat{U} .

II. The Asymptotic Behavior of ϕ_μ and U_μ

In the two limit $R \rightarrow 0$ and $R \rightarrow \infty$ the channel functions ϕ are well known and they become the eigenfunctions of ℓ_1, ℓ_2 , as the effect of $1/r_{12}$ disappears.

(a) Small R Region

At $R \rightarrow 0$ equation (9) becomes

$$\frac{\Lambda^2}{R^2} \phi_\mu = U_\mu \phi_\mu \quad (20)$$

Thus U_μ approaches the eigenvalues of Λ^2/R^2

$$U_\mu(R) \xrightarrow{R \rightarrow 0} \frac{1}{2R^2} (\ell_1 + \ell_2 + 2m_\mu + 2)^2 + 0 \left(\frac{1}{R} \right) \quad (21)$$

which represents a repulsive barrier arising from the centrifugal kinetic energy in Ω . The channel function ϕ approaches the eigenfunction of Λ^2

$$\phi_\mu = A [f_\mu(\alpha) Y_{\ell_1 \ell_2 LM}(\hat{r}_1 \hat{r}_2)] \quad (22)$$

where

$$f_{\mu} = N_{\mu} (\sin \alpha)^{\ell_1+1} (\cos \alpha)^{\ell_2+1} F(-m, \ell_1+\ell_2+2m+2 | \ell_1+\frac{5}{2} | \cos^2 \alpha) \quad (23)$$

The function F is proportional to a Jacobi polynomial of degree of m in $\cos^2 \alpha$. N is a normalization constant. The operator Λ^2 and its eigenvalues and eigenfunctions have been discussed in detail by Morse and Feshbach.

(b) Large R Region

The limit $R \rightarrow \infty$ corresponds to either $r_1 \rightarrow \infty$ or $r_2 \rightarrow \infty$. Accordingly as $R \rightarrow \infty$ one electron remains in its hydrogenic orbital at energy $E_{n_1 \ell_1}$, the other electron retains an angular momentum ℓ_2 and energy $E_{n_1 \ell_1}$ for its motion in R . Thus the asymptotic channel function is

$$\phi_{\mu} \xrightarrow{R \rightarrow \infty, \alpha \rightarrow 0} r_1 R_{n \ell_1}(r_1) Y_{\ell_1 \ell_2 LM}(\hat{r}_1 \hat{r}_2) \quad (24)$$

When putting this asymptotic channel function in hyperspherical coordinates, the analytical channel function is obtained.

APPENDIX B

The concept of oscillator strength stems from the late 19th century model of the electrical and optical behavior of matter.

A dilute gas containing N atoms per unit volume and f_s oscillators of frequency ω_s per atom, under the influence of an electric field $E_0 \exp(-i\omega t)$, has the susceptibility

$$\chi_e(\omega) = N\alpha(\omega) = N \frac{e^2}{m} \sum_s \frac{f_s}{\omega_s^2 - \omega^2 - i\gamma_s \omega} \quad (1)$$

The classical model was not developed sufficiently to determine the characteristic (spectral) frequencies ω_s and the corresponding numbers of electrons f_s . However, quantum mechanics defines the ω_s and f_s in terms of the eigenvalues and eigenfunctions of the Schrodinger equations, but that can only be accomplished approximately for many-electron atoms.

The f_s is defined in quantum mechanics as

$$f_s = \frac{2m\omega_s}{\hbar} |(z)_s|^2 \quad (2)$$

where

$$(z)_s = \langle \psi_s | \sum_i z_i | \psi_0 \rangle \quad \omega_s = \omega_s - \omega_0 \quad (3)$$

We shall assume throughout that average over the orientations of ψ_s and ψ_0 has in fact been performed.

The formulation above is called the length form for f_s . It can also be expressed in other forms. Noting that

$$\begin{aligned}
\omega_s(z_s) &= [\langle \psi_s | H | \psi_s \rangle - \langle \psi_0 | H | \psi_0 \rangle] \langle \psi_s | z | \psi_0 \rangle \\
&= \langle \psi_s | H z | \psi_0 \rangle - \langle \psi_s | z H | \psi_0 \rangle \\
&= \langle \psi_s | [H, z] \psi_0 \rangle \\
&= -i \langle \psi_s | \frac{dz}{dt} | \psi_0 \rangle \\
&= -i (P_z)_s
\end{aligned} \tag{4}$$

Substitutions of (4) in (2) yields

$$f_s = -2i(z)_s^* = \frac{2}{\omega_s} |(P_z)_s|^2 \tag{5}$$

This is called the velocity form. A further transformation gives

$$\begin{aligned}
\omega_s(P_z)_s &= \langle \psi_s | [H, P_z] | \psi_0 \rangle \\
&= -i(a_z)_s \\
&= i \left(\frac{\partial V}{\partial z} \right)_s
\end{aligned} \tag{6}$$

where

$$a_z = \sum_i a_{z_i} \quad \frac{\partial V}{\partial z} = \sum_i \frac{\partial V}{\partial z_i}$$

and a_{z_i} is the z component of the acceleration of the ith electron and V is the potential of the system hence $-\partial V / \partial z_i$ is the z component of the force applied to the ith electron by the nucleus and the other electrons. Substitution of (6) in the velocity form (5) yields

$$f_{ac} = \frac{2i}{\omega_s} (P_z)_s^* \left(\frac{\partial V}{\partial z} \right)_s = \frac{2}{\omega_s} \left| \left(\frac{\partial V}{\partial z} \right)_s \right|^2 \tag{7}$$

This is called acceleration form.

Now we shall study the formulations of oscillator strength in hyperspherical coordinates. Using equation (19) in the text for the channel

function ϕ and writing out the initial state ϕ_s and final state ϕ_p in full we have

$$\phi_s = \sum_{\ell} g_{\ell\ell}(R; \Omega) Y_{\ell\ell LM}(\hat{r}_1, \hat{r}_2) \quad (8)$$

with $L = 0$,

$$\begin{aligned} \phi_p &= \frac{1}{\sqrt{2}} \sum_{[\ell_1 \ell_2]} g_{\ell_1 \ell_2}(R; \alpha) Y_{\ell_1 \ell_2 L' M'}(\hat{r}_1, \hat{r}_2) + (-1)^{\ell_1 + \ell_2 - L' + s'} \\ &\quad g_{\ell_1 \ell_2}(R; \frac{\pi}{2} - \alpha) Y_{\ell_2 \ell_1 L' M'}(\hat{r}_1, \hat{r}_2) \\ &= \frac{1}{\sqrt{2}} \sum_{[\ell_1 \ell_2]} g_{\ell_1 \ell_2}(R; \alpha) Y_{\ell_1 \ell_2 L' M'}(\hat{r}_1, \hat{r}_2) + g_{\ell_1 \ell_2}(R; \frac{\pi}{2} - \alpha) \\ &\quad Y_{\ell_2 \ell_1 L' M'}(\hat{r}_1, \hat{r}_2) \end{aligned} \quad (9)$$

with $L'=1$.

Working in the length form we write f as

$$\begin{aligned} f &= 2\omega |\langle \psi_s | z_1 + z_2 | \psi_p \rangle|^2 \\ &= 4\omega |\int dR F_{\mu E}(R) R F_{\mu' E'}(R) \int d\Omega \phi_s \sin\alpha \sqrt{\frac{4\pi}{3}} Y_{10}(\hat{r}_1) \phi_p|^2 \\ &= 4\omega |\langle F_{\mu E} | R D_{\mu\mu'} | F_{\mu' E'} \rangle|^2 \end{aligned} \quad (10)$$

where

$$\begin{aligned} D_{\mu\mu'} &= \int d\Omega \phi_{\mu} \sin\alpha Y_{10}(1) \phi_{\mu'} \\ &= \frac{1}{\sqrt{2}} \sum_{\ell_1 \ell_2 \ell} \langle g_{\ell_1 \ell_2}(\alpha) | \sin\alpha | g_{\ell\ell}(\alpha) \rangle \\ &\quad \langle Y_{\ell_1 \ell_2 L' M'}(\hat{r}_1, \hat{r}_2) | \sqrt{\frac{4\pi}{3}} Y_{10}(\hat{r}_1) | Y_{\ell\ell LM}(\hat{r}_1, \hat{r}_2) \rangle \\ &\quad + \langle g_{\ell_1 \ell_2}(\frac{\pi}{2} - \alpha) | \sin\alpha | g_{\ell\ell}(\alpha) \rangle \langle Y_{\ell_2 \ell_1 L' M'}(\hat{r}_1, \hat{r}_2) | \sqrt{\frac{4\pi}{3}} Y_{10}(\hat{r}_1) | \\ &\quad | Y_{\ell\ell LM}(\hat{r}_1, \hat{r}_2) \rangle \end{aligned} \quad (11)$$

With the Wigner-Eckart theorem, we can calculate the matrix element of such a tensor operator \hat{Y}_{10} in the $D_{\mu', \mu}$.

$$\begin{aligned}
 & \langle Y_{\ell_1 \ell_2 L' M'}(\hat{r}_1, \hat{r}_2) | \sqrt{\frac{4\pi}{3}} Y_{10}(\hat{r}_1) | Y_{\ell \ell L M}(\hat{r}_1, \hat{r}_2) \rangle \\
 &= \sqrt{\frac{4\pi}{3}} \langle L' \| Y_1 \| L \rangle (-1)^{\ell_2} [(2\ell_1+1)(2\ell+1)]^{\frac{1}{2}} \begin{pmatrix} \ell_1 & 1 & \ell \\ 0 & 0 & 0 \end{pmatrix} \left\{ \begin{matrix} \ell_1 & L' & \ell_2 \\ L & \ell & 1 \end{matrix} \right\} \delta_{\ell_2 \ell} \\
 &= (-1)^{\ell_2} [(2\ell_1+1)(2\ell+1)]^{\frac{1}{2}} \begin{pmatrix} \ell_1 & 1 & \ell \\ 0 & 0 & 0 \end{pmatrix} \left\{ \begin{matrix} \ell_1 & 1 & \ell_2 \\ 0 & \ell & 1 \end{matrix} \right\} \delta_{\ell_2 \ell} \quad (12)
 \end{aligned}$$

where we use the double bar matrix element as

$$\begin{aligned}
 \langle L' \| Y_1 \| L \rangle &= (-1)^{L'} \left[\frac{1}{4\pi} (2L'+1)(2L'+1)(2L+1) \right]^{\frac{1}{2}} \begin{pmatrix} L' & 1 & L \\ 0 & 0 & 0 \end{pmatrix} \\
 &= \sqrt{\frac{3}{4\pi}} \sqrt{3} \begin{pmatrix} 0 & 1 & 1 \\ 0 & 0 & 0 \end{pmatrix} = \sqrt{\frac{3}{4\pi}} \quad (13)
 \end{aligned}$$

With interchange ℓ_2 and ℓ_1 we can get the second matrix element in the $D_{\mu', \mu}$

$$\begin{aligned}
 & \langle Y_{\ell_2 \ell_1 L' M'}(\hat{r}_1, \hat{r}_2) | \sqrt{\frac{4\pi}{3}} Y_{10}(\hat{r}_1) | Y_{\ell \ell L M}(\hat{r}_1, \hat{r}_2) \rangle \\
 &= (-1)^{\ell_1} [(2\ell_2+1)(2\ell+1)]^{\frac{1}{2}} \begin{pmatrix} \ell_2 & 1 & \ell \\ 0 & 0 & 0 \end{pmatrix} \left\{ \begin{matrix} \ell_2 & 1 & \ell_1 \\ 0 & \ell & 1 \end{matrix} \right\} \delta_{\ell_1 \ell} \quad (14)
 \end{aligned}$$

TABLE I

Comparison of energies for several states of He and H^- computed by this work and Pekeris et al. Energies are in atomic units.

Atom	State	Energy Eigenvalue	% Error	Reference
He	1 1S	-2.8951	0.3	-2.9037
	2 1S	-2.1400	0.28	-2.1460
	3 1S	-2.0592	0.1	-2.0613
	2 1P	-2.1214	0.1	-2.1238
	3 1P	-2.0540	0.05	-2.0551
	4 1P	-2.0301	0.02	-2.0311
H^-	1 1S	-0.5254	0.4	-0.5275

TABLE II

Comparison of f values in length and acceleration forms from this work and from Pekeris et al. for various transitions in He.

Transition	f in Len. Form	% Error	f in Acc. Form	% Error	$f(\text{Pekeris})$
$1^1\text{S}-2^1\text{P}$	0.288	4	0.334	21	0.276
3^1P	0.074	1	0.084	15	0.073
4^1P	0.030	--	0.034	13.3	0.030
<hr/>					
$2^1\text{S}-2^1\text{P}$	0.336	10.6			0.376
3^1P	0.176	16.2			0.151
4^1P	0.055	12.2			0.049
<hr/>					
$3^1\text{S}-2^1\text{P}$	-0.131	9.6			-0.145
3^1P	0.561	10.4			0.626
4P	0.171	18.7			0.144
<hr/>					

REFERENCES

1. W. L. Wiese, M. W. Smith, and B. M. Glennon, Natl. Std. Ref. Data Series, Natl. Bur. Std. U.S. 4, 1 (1966); M. L. Wiese, M. W. Smith, and B. M. Miles, Natl. Std. Ref. Data Series, Natl. Bur. Std. U.S. 22, II (1969).
2. For extensive references to past theoretical work, see R. J. S. Crossley, Advan. At. Mol. Phys. 5, 237 (1969); A. W. Weiss, Nucl. Instr. Methods 90, 121 (1970).
3. D. Miller and A. F. Starace, J. Phys. B Atom. Molec. Phys. 13 L525-L529 (1980).
4. Woodruff and J. A. Samson, Phys. Rev. A 25, 848 (1982).
5. R. P. Madden and K. Codling, Astrophys. J. 141, 364 (1965).
6. J. H. Mack, J. Phys. B 1, 831 (1968); U. Fano and C. D. Lin, in Atomic Physics 4, edited by G. Zu Puttlitz, et al. (Plenum, New York, 1975), p. 47; C. D. Lin, Phys. Rev. A 10, 1986 (1974); U. Fano, Phys. Today 29 (No. 9), 32 (1976).
7. C. D. Lin, Phys. Rev. A 29, 1019 (1983).
8. U. Fano, Rev. of Modern Phys., Vol. 40, No. 3, 441-507, July, 1968.
9. C. D. Lin, Phys. Rev. A 23, 1585 (1980).
10. B. Schiff and C. L. Pekeris, Phys. Rev. 134, A638 (1964); B. Schiff, C. L. Pekeris, and Y. Accad, Phys. Rev. A 4, 885 (1971).
11. V. I. Khvostenko and V. M. Dukelskii, Sov. Phys. JETP 10, 465 (1960).
12. J. A. R. Samon, Phys. Reports 28C, 303 (1976).
13. S. J. Smith and D. S. Burch, Phys. Rev. 116, 1125 (1959).
14. C. D. Lin, Phys. Rev. A 27, 22 (1983).

15. C. D. Lin, Phys. Rev. A12, 493 (1975).
16. D. L. Miller and A. F. Starace (unpublished).
17. H. Klarr and U. Fano, Phys. Rev. Lett. 37, 1132 (1976).
18. P. M. Morse and H. Feshbach, Methods of Theoretical Physics
(McGraw-Hill, New York, 1953) p. 1755. (1953)
19. S. Chandrasekhar, Astrophys. J. 102, 223 (1945).

THEORETICAL STUDY OF OSCILLATOR
STRENGTH IN HYPERSPHERICAL COORDINATES

by

JIANG TAN
B.A., Cherkang University, 1976

AN ABSTRACT OF A MASTER'S THESIS

submitted in partial fulfillment of the
requirements for the degree

MASTER OF SCIENCE

Department of Physics

KANSAS STATE UNIVERSITY

Manhattan, Kansas

1985

ABSTRACT

On the basis of adiabatic approximation in hyperspherical framework the oscillator strength f and the photo-absorption cross sections of 2-electron systems, He and H^- , are calculated. In particular both the length form and acceleration form of oscillator strength are computed. The adiabatic wave functions employed in the f calculations and the disagreement between the results calculated from the two f forms are discussed qualitatively. Some details on comparison with experimental data and other theoretical results are given.